

## Fringing field effects on electrical resistivity of semiconductor nanowire-metal contacts

Jun Hu,<sup>1,a)</sup> Yang Liu,<sup>2</sup> C. Z. Ning,<sup>3</sup> Robert Dutton,<sup>2</sup> and Sung-Mo Kang<sup>4</sup>

<sup>1</sup>Baskin School of Engineering, University of California, 1156 High Street, Santa Cruz, California 95064, USA

<sup>2</sup>Integrated Circuits Laboratory, Stanford University, Stanford, California 94305, USA

<sup>3</sup>Center for Nanophotonics and Department of Electrical Engineering, Arizona State University, Tempe, Arizona 85287, USA

<sup>4</sup>School of Engineering, University of California, Merced, 5200 North Lake Road, Merced, California 95343, USA

(Received 16 December 2007; accepted 4 February 2008; published online 27 February 2008)

Metal contacts play an important role in nanowire devices and are expected to exhibit qualitatively different properties from those of planar contacts due to small contact cross sections. We numerically investigate certain unique properties of nanowire-metal contacts and demonstrate that contact resistivity increases as nanowire radius shrinks. This increase is more significant for nanowire-three-dimensional metal contacts than for nanowire-one-dimensional metal contacts. The underlying cause for this size effect is identified as the strong fringing field effects, which become more significant as temperature decreases. Our simulation provides a more complete understanding of the size effects on nanowire-metal contacts. © 2008 American Institute of Physics.

[DOI: 10.1063/1.2889534]

Semiconductor nanowires (NWs) are a subject of great interest since they are expected to extend, or to enhance complementary metal-oxide semiconductor technology, and to lead to more efficient nanoscale optoelectronic devices. So far, extensive wire growth and device fabrications have been performed and different functionalities have been demonstrated ranging from lasers,<sup>1</sup> transistors,<sup>2,3</sup> and logic circuits.<sup>2</sup> The resistance of NW-metal contacts is a key parameter that affects the electrical injection efficiency, and ultimately, the device performance. Some progresses have been reported recently in synthesizing such contacts with low contact resistivity.<sup>4-8</sup> However, a complete understanding of the NW-metal contacts is still lacking. Such an understanding of the contact physics can be very useful for the improvement of contact designs. It is to be noted that the classical semiconductor-metal contact theories<sup>9</sup> assume bulk condition, and cannot be readily applied to the case of NW-metal contacts, where the finite cross sections of NWs need to be taken into account. Recently, size-dependent effects on electrical contacts to nanotubes and NWs were studied<sup>10</sup> for the case of side contact geometry, where semiconductor cores were surrounded by metal electrode shells. In that case, the size-dependent effects were due to the limited available depletion width in the radial direction. Conductivity of thin wires was also investigated by considering different boundary conditions of Ohmic and Schottky contacts,<sup>11</sup> where contact resistivity associated with the thermally excited tunneling process was not included in their analytical derivation. In this work, we numerically investigated the size effects on contact resistivity for the end contact geometry, where the ends of NWs are attached to metal electrodes. The small cross section of NW-metal contact is expected to cause weak screening and strong fringing field effects that are absent in planar contacts between a bulk metal and a large semiconductor. Similar effects have been previously investigated on

the depletion width and tunneling conductance dependence on doping density for nanotube based  $p$ - $n$  junctions.<sup>12</sup> The role of the contact geometry has been previously studied for nanotube based Schottky barrier transistors;<sup>13</sup> it has been pointed out that needlelike one-dimensional (1D) contacts lead to lower resistances and turn-on gate voltages. In this work, we quantitatively study the unique properties of NW-metal contacts and particularly the role of wire radius and depletion length, which is important to guide the design and fabrication of NW-based electronic and optoelectronic devices.

In this letter, we numerically investigate two different NW-metal contact geometries, as schematically shown in Fig. 1: (a) NW-three-dimensional (3D) metal contact, where the metal cross section is much larger than that of the NW and (b) NW-1D metal contact, where the metal and the NW have equal cross section.<sup>11</sup> For these two contact geometries, we will examine the contact resistivity dependence on wire radius, as well as on temperature and Schottky barrier height, and compare the results with planar contact [Fig. 1(c)]. The underlying cause for such size effect will also be examined.

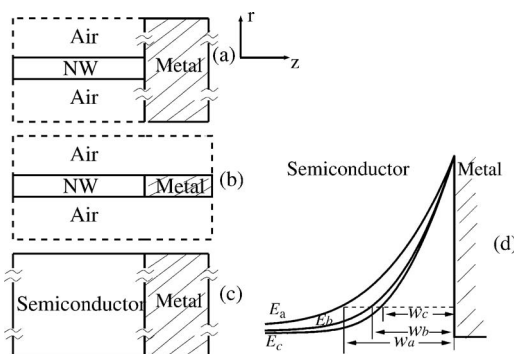


FIG. 1. Contact geometries studied in the paper (a) NW-3D metal contact, (b) NW-1D metal contact, (c) planar contact. (d) shows simulated energy band diagrams for different contact geometries.

<sup>a)</sup>Electronic mail: hujun@soe.ucsc.edu.

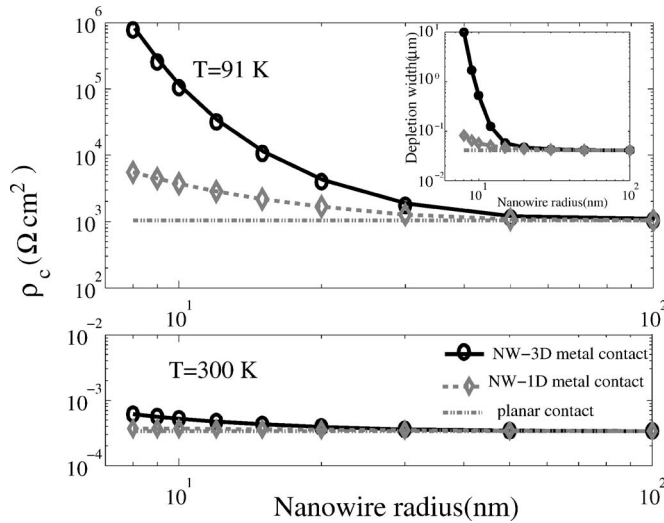


FIG. 2. Contact resistivity vs NW radius for different contact geometries at temperatures equal to 91 and 300 K, respectively. The inset shows the depletion width vs NW radius.

We employ a general device simulator, Prophet,<sup>14</sup> to numerically solve the Shockley semiconductor equations to obtain energy band diagrams. Then, the contact resistivity  $\rho_c$  is calculated in a postprocessing step using the numerical model in Ref. 15. Our numerical results for contact resistivity of planar silicon-metal contacts were verified against analytical results in Ref. 16. The detailed calculation process is given below.

The total current in a metal semiconductor contact is composed of both the thermionic emission current ( $J_{th}$ ) and the thermionic-field (TF) emission current ( $J_t$ ) caused by thermally excited tunneling,<sup>17</sup> i.e.,  $J = J_{th} + J_t$ . For the cases studied in this paper, the thermionic emission current is found to be much smaller than the TF emission current. We focus our analysis on the dominant TF emission current, which is given by (Ref. 17)

$$J_t = \frac{A^* T}{k} \int_0^\infty \tau(E) \exp[-(E + q\phi_s)/kT] dE \times [1 - \exp(-qV_f/kT)], \quad (1)$$

where  $A^*$  is the Richardson constant,  $k$  is the Boltzmann constant,  $T$  is temperature, and  $E$  is the conduction band edge energy.  $\tau(E)$  is the tunneling probability for carriers,  $V_f$  is the applied forward bias, and  $q\phi_s$  is the potential energy of the charge carriers relative to the Fermi energy in the semiconductor.

This current can be calculated once the energy diagram is obtained from the simulations and the contact resistivity  $\rho_c$  is calculated as  $\rho_c = (\partial J / \partial V)^{-1}|_{V=0}$ .<sup>18</sup> The simulations are two dimensional ( $r$  and  $z$ ) assuming rotational symmetry. Long GaAs NWs surrounded by ambient dielectric materials (air in this work) are simulated as an example. The doping density is  $5 \times 10^{17} \text{ cm}^{-3}$  and the Schottky barrier height is 0.4 eV unless otherwise specified. The exact value of wire length is not important, but chosen to be  $95 \mu\text{m}$  for specificity.

Figure 1(d) shows simulated energy band diagrams for different contact geometries. It clearly shows different depletion widths  $w$  for different contact geometries. We plotted the depletion width dependence on NW radius in the inset of Fig. 2. It is shown that as NW radius shrinks, the depletion

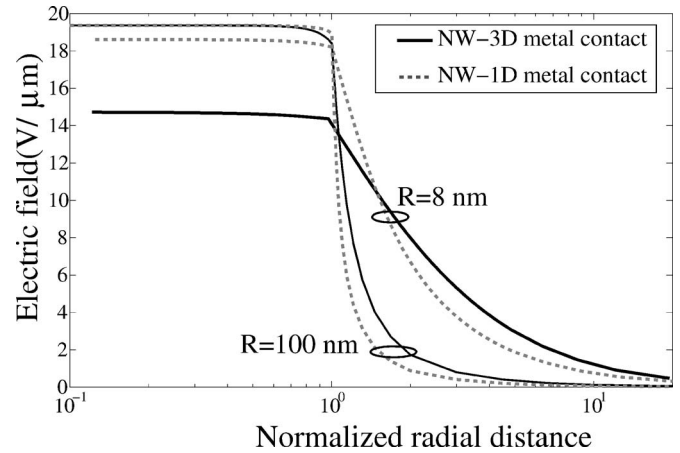


FIG. 3. Longitudinal electric field in the radial direction (distance normalized by wire radius) for different NW radii:  $R=8 \text{ nm}$  and  $R=100 \text{ nm}$ .

width increases. This increase is more abrupt in NW-3D metal contacts than in NW-1D metal contacts. The constant depletion width value of planar contacts is also shown. Here, depletion width is defined as the distance from the NW-metal interface where the charge drops to 90% of the charge in depletion region. Such size effect is associated with the finite cross sections of NWs.

In Fig. 2, we investigated the dependence of contact resistivity on NW radius due to the depletion width variation. The contact resistivity for NWs is calculated by ignoring the radial variation of energy band diagram since this variation is negligible, as shown in Fig. 3. The results indicate that the contact resistivity increases as NW radius shrinks. This increase is more significant for NW-3D metal contacts than for NW-1D metal contacts and at low temperature than at high temperature. We also note that the contact resistivity can increase by more than three orders of magnitude for a NW-3D metal contact at low temperature. The contact resistivity against wire radius variation is more stable for NW-1D metal contacts than for NW-3D metal contacts.

Equation (1) shows that for different contact geometries, the origin of  $J_t$  variation is the occupation probability in the semiconductor,  $\exp[-(E + q\phi_s)/kT]$ , and the tunneling probability for carriers,  $\tau(E)$ . As shown in Fig. 1(d), at low temperature, the occupation probability is very small in high energy region and thermally excited tunneling happens mostly at the low energy part of the Schottky barrier. In this region, the difference in depletion width  $w$  for different contact geometries is significant. Furthermore, different  $w$  values are reflected more significantly in  $\tau(E)$ . Hence, the thermally excited tunneling current is dramatically different for different contact geometries. At high temperature, the term  $\exp[-(E + q\phi_s)/kT]$  is still large in high energy regime due to high temperature  $T$  and thermally excited tunneling happens mostly around the top of the Schottky barrier. In this region, the difference in  $w$  for different contact geometries is much smaller. So the contact resistivity increase is less significant as NW radius decreases in high temperature case.

To understand the origin of the depletion width dependence on NW radius, we studied the longitudinal component of electric field ( $E_z|_{z=z_1} = -\partial\phi/\partial z$ , where  $z_1$  is close to the NW-metal interface), and plotted this field profile along the radial direction for NW-3D metal contacts and NW-1D metal contacts (Fig. 3). It demonstrates that fringing field is strong

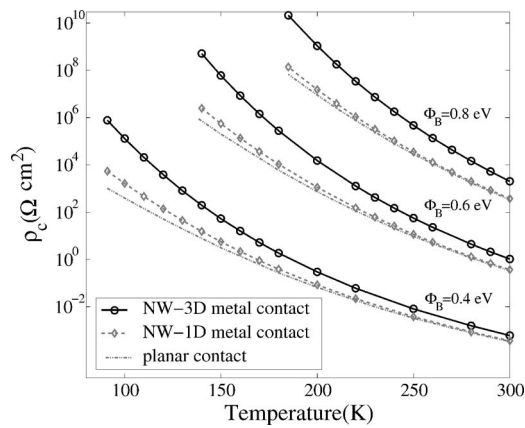


FIG. 4. Contact resistivity vs temperature for different values of Schottky barrier height  $\Phi_B$ . Wire radius is 8 nm for NW-metal contacts.

and screening in the wire is weak for NWs with small radii (e.g., 8 nm). This makes the electric field lines incline to the ambient around the wires, which leads to weaker electric field inside the wires. The reduced electric field in the wires results in larger depletion width, smaller tunneling current, and larger contact resistivity. It is also apparent from Fig. 3 that the fringing field effects are more significant in NW-3D metal contacts than in NW-1D metal contacts for NWs with small radii. For NWs with large radii (e.g., 100 nm), the fringing field effects become less significant.

For completeness, we studied the fringing field effects on contact resistivity for different barrier heights  $\Phi_B$ , at different temperatures (Fig. 4). The results show that for a given temperature, the difference in contact resistivity for different contact geometries is more significant in higher barrier height cases than in lower barrier height cases. This is because for a given temperature, the higher the barrier is, the more likely thermally excited tunneling happens at the lower energy part of the Schottky barrier. To conclude, the fringing field effects have great impact on contact resistivity at low temperatures for higher barrier height cases and this impact becomes negligible when temperature is high enough. Figure 4 provides guide to the correct estimation of contact resistivity for different Schottky barrier heights at different temperatures for NW-metal contacts. We note that so far our study has been mostly aimed at applications of NW-based two-terminal optoelectronic devices, such as light-emitting diodes, lasers, and photodetectors. It has already been shown that for nanotube based transistors, the gate electrodes play a very important role in determining the contact resistance.<sup>13</sup> This is because for 1D systems, the increased length of contact depletion region tends to result in its significant overlap

with the gate-controlled channel region. The study of the role of gate electrode in NW-based transistors is left for future work.

We have shown that the depletion width and contact resistivity for NW-metal contacts increase as NW dimension shrinks due to strong fringing field effects, and this effect is significant in NW-3D metal contacts at low temperatures. Using this observation, we explained why NW-1D metal contacts are much better than NW-3D metal contacts, especially at low temperatures; NW-1D metal contacts are less sensitive to NW radius variation and the contact resistivity for NW-1D metal contacts are much smaller than that of NW-3D metal contacts. Our work provides guidance to the correct estimation of contact resistivity, which is useful for NW device design and fabrications.

The work was supported by grants from NASA Ames Research Center through the University Affiliated Research Center Aligned Research Program. The authors also appreciate the partial support from the MARCO Focus Center Research Program in modeling for optical interconnects (IFC) and device scaling issues of NWs (MSD).

- <sup>1</sup>X. F. Duan, Y. Huang, R. Agarwal, and C. M. Lieber, *Nature (London)* **421**, 241 (2003); M. Huang, S. Mao, H. Feick, H. Yan, Y. Wu, H. Kind, E. Weber, R. Russo, and P. Yang, *Science* **292**, 1897 (2001); J. C. Johnson, H. J. Choi, K. P. Knutsen, R. D. Schaller, P. Yang, and R. J. Saykally, *Nat. Mater.* **1**, 102 (2002); A. H. Chin, S. Vaddiraju, A. V. Maslov, C. Z. Ning, M. K. Sunkara, and M. Meyyappan, *Appl. Phys. Lett.* **88**, 163115 (2006).
- <sup>2</sup>Y. Huang, X. Duan, Y. Cui, L. Lauhon, K. Kim, and C. M. Lieber, *Science* **294**, 1313 (2001).
- <sup>3</sup>P. Nguyen, H. T. Ng, T. Yamada, M. K. Smith, J. Li, J. Han, and M. Meyyappan, *Nano Lett.* **4**, 651 (2004).
- <sup>4</sup>E. Stern, G. Cheng, M. P. Young, and M. A. Reed, *Appl. Phys. Lett.* **88**, 053106 (2006).
- <sup>5</sup>E. Stern, G. Cheng, J. F. Klemic, E. Broomfield, D. Turner-Evans, C. Li, C. Zhou, and M. A. Reed, *J. Vac. Sci. Technol. B* **24**, 231 (2006).
- <sup>6</sup>J. S. Hwang, D. Ahn, S. H. Hong, H. K. Kim, S. W. Hwang, B. H. Jeon, and J. H. Choi, *Appl. Phys. Lett.* **85**, 1636 (2004).
- <sup>7</sup>W. Wu, J. B. DiMaria, H. G. Yoo, S. Pan, L. J. Rothberg, and Y. Zhang, *Appl. Phys. Lett.* **84**, 966 (2004).
- <sup>8</sup>D. Erts, B. Polyakov, B. Daly, M. A. Morris, S. Ellingboe, J. Boland, and J. D. Holmes, *J. Phys. Chem.* **110**, 820 (2006).
- <sup>9</sup>S. M. Sze, *Physics of Semiconductor Devices*, 2nd ed. (Wiley, New York, 1981).
- <sup>10</sup>F. Leonard and A. Alec Talin, *Phys. Rev. Lett.* **97**, 026804 (2006).
- <sup>11</sup>H. Ruda and A. Shik, *J. Appl. Phys.* **84**, 5867 (1998).
- <sup>12</sup>F. Leonard and J. Tersoff, *Phys. Rev. Lett.* **83**, 5174 (1999).
- <sup>13</sup>S. Heinze, J. Tersoff, R. Martel, V. Derycke, J. Appenzeller, and Ph. Avouris, *Phys. Rev. Lett.* **89**, 106801 (2002).
- <sup>14</sup><http://www-tcad.stanford.edu/prophet/>.
- <sup>15</sup>Y. Liu, e-print arXiv:0802.0729.
- <sup>16</sup>K. K. Ng and R. Liu, *IEEE Trans. Electron Devices* **37**, 1535 (1990).
- <sup>17</sup>C. R. Crowell and V. L. Rideout, *Solid-State Electron.* **12**, 89 (1969).
- <sup>18</sup>H. H. Berger, *J. Electrochem. Soc.* **119**, 507 (1972).